Localisation effects on the Vibron Shifts in Helium-Hydrogen Mixtures

Localisation Effects on the Vibron Shifts in Helium-Hydrogen Mixtures

Sam B. Ramsey, Miriam Pena-Alvarez, and Graeme J. Ackland
Centre for Extreme Conditions, School of Physics and Astronomy, The University of Edinburgh, Edinburgh EH9 3FD
(Dated: April 16, 2020)

The vibrational frequency of hydrogen molecules has been observed to increase strongly with He concentration in helium hydrogen fluid mixtures. This has been associated with He-H interactions, either directly through chemical bonding[1], or indirectly through increased local pressure[2]. Here, we demonstrate that the increase in the Raman frequency of the hydrogen molecule vibron is due to the number of H_2 molecules participating in the mode. There is no chemical bonding between He and H_2, helium acts only to separate the molecules. The variety of possible environments for H_2 gives rise to many Raman active modes, which causes broadening the vibron band. As the Raman active modes tend to be the lower frequency vibrons, these effects work together to produce the majority of the shift seen in experiment. We used Density Functional Theory (DFT) methods in both solid and fluid phases to demonstrate this effect. DFT also reveals that the pressure in these H_2-He mixture is primarily due to quantum nuclear effects, again the weak chemical bonding makes it a secondary effect.

I. INTRODUCTION

Hydrogen and helium are the simplest and most abundant elements in the universe. As such the recent claim that there is chemical bonding between hydrogen and helium is potentially transformative to understanding their high pressure interactions for both the condensed matter and astrophysical communities[1]. The lightness of each element means that nuclear motion and zero-point effects play a large part in their dynamics, so that standard methods of electronic structure calculation are insufficient to describe them. This gives rise to exotic phases of matter such as superfluids and, potentially, supersolids[3,4]. Understanding mixtures of hydrogen and helium under pressure is important for the study of the gas giants such as Jupiter and Saturn as they are the primary constituents[5–7]. It is also important to characterise the mixtures as helium is commonly used as a pressure medium in diamond anvil cell (DAC) experiments[8].

Helium and molecular hydrogen are readily miscible in the fluid regime. DAC experiments <10 GPa see a single fluid phase with the characteristic signal being the Raman active mode of the hydrogen vibron[9]. The vibron frequency is seen to be blueshifted in mixtures, with the magnitude of this shift being dependent on the relative concentration of the mixture. This has been variously attributed to an effective increase of pressure induced on the hydrogen molecule due to the helium solution[2,9] although no amount of pressure can cause such a large shift in pure hydrogen, and to novel chemical bonding[1]. At higher pressures, first H_2 and then He solidify into hexagonal close-packed solids and demix, perhaps causing "He-rain" (or more properly, snow) in planetary atmospheres. Weak H_2 vibrons have been observed in the He-rich solid[1], suggesting low solid solubility.

Helium and hydrogen have been known to form stable alloys with other Noble gases[10–13]. A similar frequency shift is seen in the Raman spectrum of the hydrogen compounds. This suggests that the effect is caused by coupling between hydrogen molecules weakening as they are separated by the chemically inert elements[14–16]. A simple classical molecular potential with nearest neighbour interactions has shown that this effect is of the right order of magnitude to explain the behaviour in Argon-hydrogen mixtures[14,17]. To our knowledge no theoretical work has addressed this effect in helium-hydrogen mixtures. Here we present a first-principles investigation of this effect to accurately describe the observed experimental effects.

II. METHODS

To study the system, density functional theory calculations were carried out on mixtures of helium and hydrogen at various concentrations. Previous work has concentrated on astrophysically relevant conditions, <100 GPa and <1000 K, where van der Waals interactions and nuclear quantum effects can be safely ignored[7,18,19]. Our calculations are at relatively low pressures and require van der Waals interactions, which are accounted for using a Grimme dispersion scheme and a PerdewBurke-Ernzerhof functional[20–22]. Moreover, below 5 GPa, the largest contribution to the pressure comes from quantum nuclear effects: the pressure arising from changes in zero point energy (ZPE) with density. To account for this we carry out standard Nose-Parrinello-Rahman (NPT) calculations, as implemented in CASTEP[23], then use lattice dynamics and the quasiharmonic approximation to calculate the true pressure. There is no analytic form for the variation of the zero-point energy with volume within DFT. So in practice, this required calculating the free energy as a function of volume and temperature $G(V,T)$, for cells relaxed in the NPT ensemble to have isotropic stress and including the zero point energy. We then perform a numerical Legendre Transform on the grid of $G(V,T)$ to obtain $G(P,T)$.

We used molecular dynamics calculation to model the fluid state, and used geometry optimized hexagonal close

packed (HCP) lattice for the solid. Hydrogen molecules and He atoms were randomly distributed to produce various concentrations with all molecular dynamics calculations being carried out at 300 K.

Several thousand molecules are required to fully describe the liquid structure[24], but the phonon density of states is well sampled in much smaller cells. Density functional perturbation theory (DFPT) was used to calculate Raman activity and the vibrational contribution to the pressure. Simulation cells of 36 molecules were used for both fluid and solid regimes. To capture the disordered structure of the fluid regime molecular dynamics calculations were carried out for 1 ps at 300 K before snapshots were taken. 5 snapshots were taken from each molecular dynamics run to ensure proper sampling of atomic configurations. The resulting snapshots were then relaxed to a local minimum so that DFPT calculations could be carried out[40]. This allowed us to simulate the hydrogen vibron, which occurs over relatively short time scales, including the effects of the disordered fluid without the computational cost of large molecular dynamics simulations. The enthalpy was converged to 1 meV using a 2x2x2 kpoint grid. Van der Waals functionals are essential for helium, however, it is also well known that these functionals overestimate the hydrogen vibron frequency[25]. To facilitate comparison with the experimental, calculated frequencies are shifted by 126 cm^{-1} to match the experimental hydrogen vibron. The high pressure calculations shown in the inset of Fig. 2 were carried out using simulation cells of 96 molecules and a 3x3x3 kpoint grid. All calculations are carried out using the CASTEP code[23].

III. RESULTS AND DISCUSSION

While solid helium at these pressures has been well studied using classical potentials no previous studies using standard DFT have been published. Ab-initio methods have the advantage of reliably working with multiple elements over a wide range of pressures[26,27]. Fig. 1 demonstrates that whilst Van der Waals effects are important, the dominant contribution to the pressure comes from quantum nuclear effects, and that . These have a massive effect on the equation of state, shifting the equilibrium density in pure He by about 50%.

The effect of increasing He concentration in these calculations is to blueshift the vibron and to reduce the ZPE pressure. In Fig. 2, the calculated frequencies at different He concentrations at different pressures are presented together with experimental results[1,28]. The frequencies changes are in good agreement with the experimental results. Analysis of the vibron eigenmodes shows negligible participation of the He atoms in the motion, demonstrating the absence of chemical interactions between helium and hydrogen. This suggests the observed *blueshift* with increasing helium concentration is due to fewer couplings between adjacent H_2 molecules and localisation of the vibrational modes.

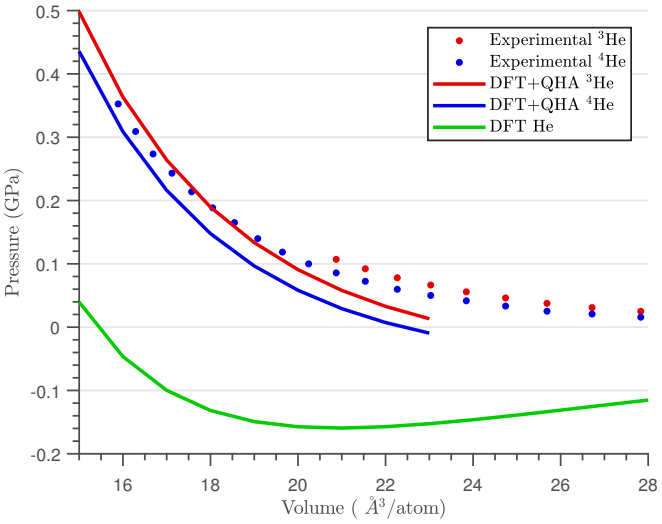

FIG. 1: Equation of state of both helium isotopes in the HCP structure. The DFT calculations use Grimme van der Waals corrections, for which HCP is stable against BCC and FCC. The green line shows the equation of state in the Born-Oppenheimer approximation. Blue and red curves show the effect of adding zero-point pressures in the quasiharmonic approximation. Above 20 $Å^3$/atom the static relaxations give negative pressure, and above 23 $Å^3$/atom the HCP structure cannot be stabilized without ZPE. Experimental data are from X-ray and strain gauge measurements[29–32].

.

	ΔH (eV)	ΔE (eV)	Miscibility
Substitutional	0.164	0.048	0.2%
Tetrahedral	0.552	1.267	2x10^{-7}%
Octahedral	0.640	1.032	5x10^{-6}%

TABLE I: The enthalpy and energy cost of including hydrogen atoms in HCP helium at 12 GPa for each site is given. The miscibility ($e^{-\Delta H/kT}$) at 300 K is calculated assuming a dilute regular solid solution.

To determine miscibility within the solid regime we examined H_2 impurities in helium. Both hydrogen and helium atoms form HCP solid phases in this pressure regime, and the enthalpy of solution means hydrogen can only occupy substitutional sites in the solid helium lattice (Table I). At room temperature, the calculated solubility limit is 0.2%. This is in keeping with the existing literature[6,7,33,34]. Measuring such a small concentration experimentally is challenging: a weak vibron signal in the He-rich fluid has been noted[1], but another recent paper shows no signal[35] despite indicating solubility up to 10% (Fig. S1 in that paper).

Table II shows the binding energy for clusters of substitutional hydrogen molecules compared with isolated hydrogen molecules in solid helium. All the enthalpies of formation are negative, and become larger as more hydrogen is added, a strong suggestion that when within a helium lattice, hydrogen molecules tend to cluster as they

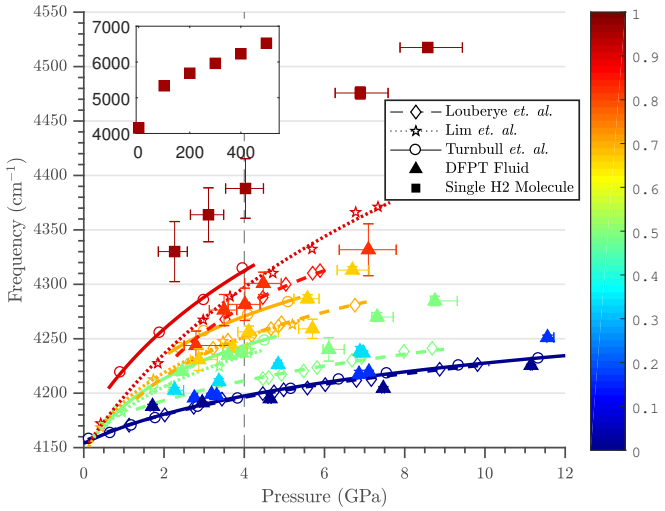

FIG. 2: Comparison of experimental and calculated pressure-frequency relation with color-coding used to show the atomic fraction of Helium (X_{He}). The color scale is represents the concentration of helium: only data of the same color should be compared. The lowest helium concentrations shown are pure hydrogen and the highest have a single hydrogen molecule in the simulation cell. Experimental data taken from Turnbull *et. al.*[28], Lim *et. al.*[1], and Loubeyre *et. al.*[9] is plotted against DFT results from the fluid regime for a range of concentrations and pressures. All experimental data are fitted with a logarithmic function. A more direct comparison of concentration and frequency is given in Fig. 3. The Raman and phonon density of states shown in Fig. 3 are taken at 4 GPa as denoted by the grey vertical line. The inset shows the frequency of the isolated hydrogen molecule vibron up to 500 GPa. All frequencies have been shifted by 126 cm^{-1} to account for the functionals over-binding of hydrogen molecules[25]. Pressures and horizontal error bars are found by fitting each concentration to a Birch-Murnaghan equation of state. Vertical error bars are simply the standard deviation of the 5 samples taken from each molecular dynamics calculation.

	ΔE	ΔE+ZPE(eV)	$k_BT \ln N$
Pair	-0.043	-0.006	0.017
Triplet	-0.114	-0.023	0.025
Quadruplet	-0.185	-0.037	0.034

TABLE II: Formation energy for clusters of substitutional hydrogen molecules compared with a lone hydrogen molecule in an HCP helium lattice. Results with and without accounting for zero-point energy are shown, along with the configurational entropy cost to the free energy at room temperature.

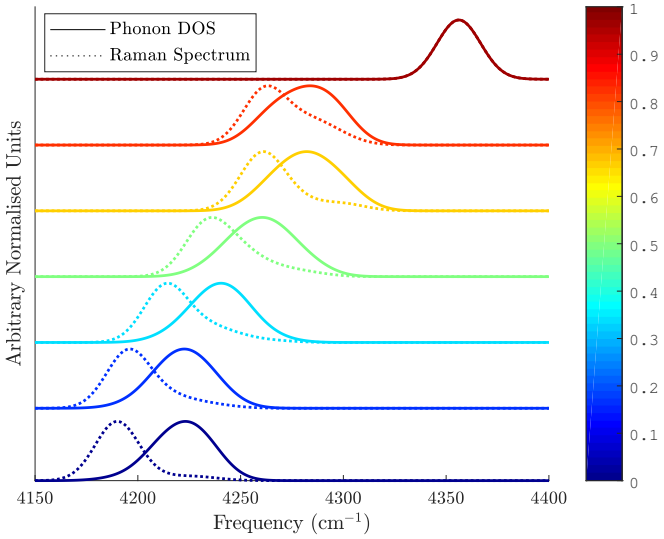

FIG. 3: Phonon density of states and associated Raman intensities for a range of concentrations is taken from DFPT calculations carried out in the fluid model showing how the hydrogen vibron mode changes with concentration (colorbar shows He concentration). The phonon density of states broadens and the average frequency blueshifts shifts as the He concentration is increased. As the strongest Raman active mode is the lowest frequency of the phonon band this results in the Raman intensities diverging from the phonon density of states at lower He concentration. Weaker Raman modes give a pronounced high frequency "tail" to the Raman peak. All peaks fitted with a 25 cm^{-1} FWHM Gaussian broadening. These spectra have been taken at 4 GPa as indicated by the grey doted line in Fig 2.

attract one another. Standard DFT calculations suggest strong H_2-H_2 interactions, relative to He-He, but unexpectedly this difference is significantly reduced when the ZPE is accounted for through DFPT. Nevertheless, below room temperature the binding is close to the configurational entropy cost, so significant numbers of H_2 microclusters can be expected. The vibrons associated with H_2 solutes are significantly blueshifted from the pure H_2 value due to the lack of coupling, with the single substitutional having the largest shift, perhaps accounting for the multiple Raman peaks attributed to interstitials by Yoo *et al.*[1].

Recent experimental results have claimed that at room temperature and pressures above 12 GPa helium and hydrogen are able to chemically bond[1,36]. The experimental evidence for chemical association comes from another vibrational mode observed at around 2400 cm^{-1}. We do not see any evidence of any vibrational modes in this frequency range in our calculations. Other studies[28,34] have demonstrated that this effect could be due to nitrogen contamination. If, as we propose, the concentration dependence is due simply to the number of hydrogen's participating in the modes, then the effect will be largely independent of whether the hydrogen is diluted by He or N_2: by contrast whereas He-H_2 chemical bonding or local stresses[2] will depend on the composition of the solvent. The experiments show consistent vibron shifts with H_2 concentration, regardless of nitrogen content[1,28].

As shown by Fig. 2, an isolated hydrogen molecule, (represented by the $X_{He} = 0.9722$), in a helium mixture has a significantly higher Raman frequency than pure hydrogen at the same pressure. Fig. 3 shows that as X_{He} concentration decreases the phonon density of states band is both *broadened* and *shifted*. The apparent phonon frequency shift due to concentration is en-

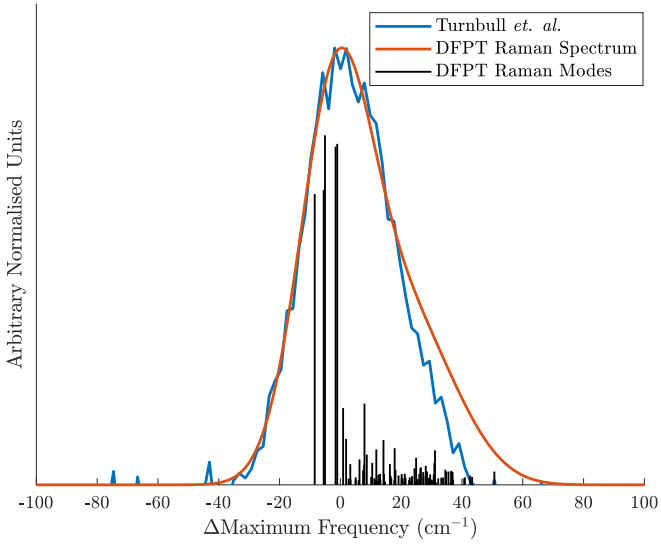

FIG. 4: Comparison of experimental Raman peak with DFT data at 2.7 GPa and 50% H_2 concentration. The DFPT Raman intensities shown in black are convolved with a 28 cm^{-1} Gaussian broadening to get the resulting spectrum. Blue experimental data were collected during a previous campaign[28]. Both the experimental and DFT spectra are asymmetric with a high frequency tail. This effect is due to the weaker, but still active, Raman modes at higher frequency. Raman modes from all 5 snapshots taken at this pressure shown in the figure.

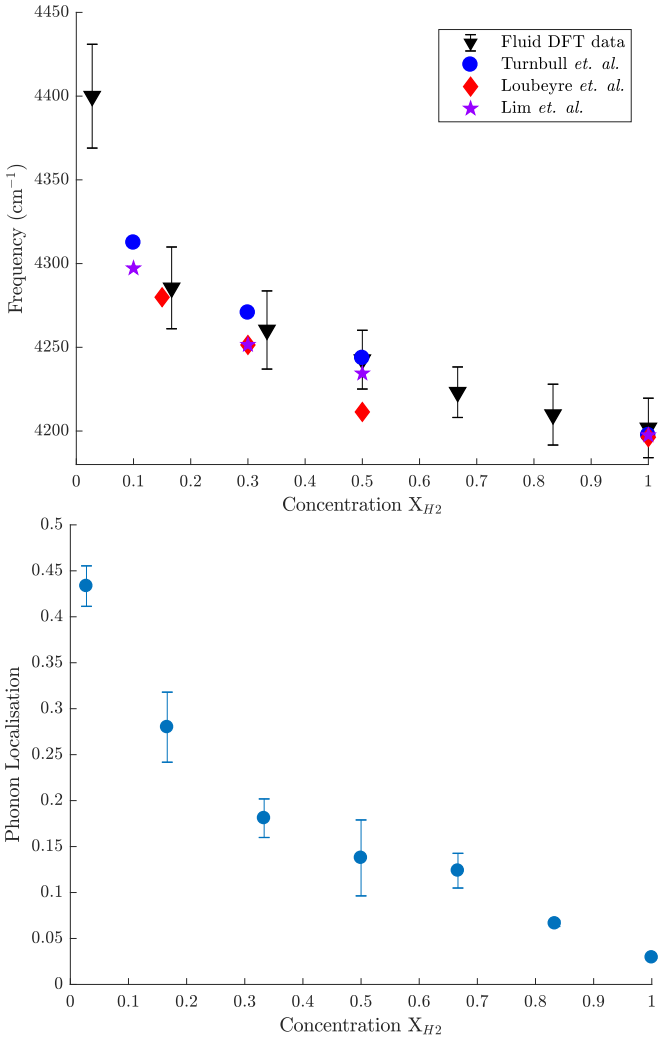

FIG. 5: (a) DFPT calculation plotted against experimental results[1,9,28], showing the change in Raman active vibron due to change in mixture composition at 4 GPa. DFPT frequencies at precisely 4 GPa are interpolated from data shown in Fig. 2. Error bars on DFPT data are taken from the RMSE of the fits to data in Fig. 2. (b) Calculations of the inverse participation ratio of the calculated strongest Raman-active phonon modes. The error bars are taken from the standard deviation of three independent configurations in the solid regime at each concentration.

hanced by the broadening (Fig. 5), because Raman activity tends to be stronger for the lower frequency vibron modes. DFPT calculations in the fluid reveal that even the Raman the peak arises from several modes. The in-phase vibration of all molecules in a cluster is the strongest, but in the absence of symmetry many other modes acquire some Raman activity. These modes have slightly higher frequency than the in-phase vibron, so cause a skew in the peak shape Fig. 4.

Comparison of the panels in Fig. 5 provides strong evidence that the frequency shift is due to localization, which we measure as the inverse participation ratio:

$$\frac{\sum_i \mathbf{e}_i^4}{(\sum_i \mathbf{e}_i^2)^2}$$

where $\mathbf{e}_i$ is the mode displacement vector of each atom i. The larger the number of hydrogen atoms participating in a vibron mode, the lower its frequency. An isolated hydrogen molecule has the highest frequency, while the lowest observed mode occur in pure solid hydrogen, where the Raman mode involves all molecules vibrating together. The shift and multiplicity of the peaks due to species and fluid disorder are similar to the isotope disorder effect in hydrogen[37,38].

These effects are seen in both the solid and the fluid, However, the solid vibron shift is larger because the pure H_2 fluid vibron is already partially localised due to the disordered nature of the fluid. At high H_2 concentrations the differences between solid and fluid are largest: all hydrogens have many coupled neighbours, but the fluid vibron is still localised due to the disorder.

The comparison with the experimental fluid measurements shows that the main effects of involved in the frequency shift are qualitatively reproduced in this model. The primary experimental evidence of solid phase miscibility is observation of an H_2 vibron mode in the helium[1]. Consistent with our calculations for *substitutional* and *clustered* H_2, these observed modes are blueshifted with the less-blueshifted cluster mode being broader. It was not possible to determine a precise H_2 concentration in the experiment[41], but our calculated solubility is suffi-

cient to produce an observable signal and therefore the calculations support the experimental data[1].

In our DFPT calculations we have assumed that two elements are randomly distributed throughout the mixtures. However, if the hydrogen molecules are more clustered this would enhance coupling and drive down the vibron frequency of the high X_{He} mixtures. To understand the potential magnitude of this effect DFPT calculations were carried out on a simulation cell with $X_{He} = 0.8333$ with a single cluster of hydrogen molecules: This resulted in a drop in frequency of 22 cm^{-1}, and reduced inverse participation ratio. Thus we show that localization increases the frequency, independent of concentration.

Our results may serve as a reference for future works on mixtures and alloys in general, and on hydrides in particular. Experimental mixtures are sometimes prepared *in situ* and the real concentration of the components may not be known. However, here we show that a relationship between Raman shift, pressure and hydrogen concentration which could be used as a reference concentration calibrations. On the other hand, this work highlights that attention should be paid not only to the shifting of the vibrons but also to the width as it can provide important information about concentrations and inter molecular interactions. Here we characterise a system in which a hydrogen molecule can be confined without chemical interaction. These isolated hydrogen molecules act as an analogy for a confined hydrogen molecule which may in future be compared directly to experiment. As shown in the inset of Fig. 2 the frequency of the isolated hydrogen molecule in the helium pressure medium continues to increase as the pure hydrogen's frequency decreases. This demonstrates the importance of coupling effects even at higher pressures.

IV. CONCLUSIONS

In conclusion we have carried out the first ab-initio study of the hydrogen molecular vibron in HeH_2 mixtures. We show that including van de Waals corrections and zero point energy effects are essential to reproducing the equation of state below 10 GPa. The vibron blueshift with increasing He concentration is shown to be due to the reduction of hydrogen-hydrogen coupling and the associated localisation of the vibrational mode. "local pressure" effects can be ruled out because the isolated hydrogen molecule in He has a significantly higher vibron frequency than pure hydrogen at any pressure. The observed broadening of the vibron in mixtures is because there are Raman active vibrations involving various numbers of H_2 atoms. The calculations support the possibility of small amounts of H_2 existing as substitutional impurities in solid He, but unequivocally rule out interstitial H_2 or any He-H_2 chemical bond.

Acknowledgments

We acknowledge E.Gregoryanz and R.Howie for useful discussions and for sharing their primary data, and C.S.Yoo regarding the observability of low H_2 concentrations in the He-rich fluid. GJA and MPA were supported by the ERC Hecate project, and SBR acknowledges a studentship from EPSRC. Computing resources were provided by UKCP (EPSRC grant EP/P002790). Since this work was completed, some results in this paper regarding solid phases at 0K have been replicated elsewhere.[39].

[1] J. Lim and C.-S. Yoo, Phys. Rev. Lett. **120**, 165301 (2018).
[2] P. Loubeyre, R. Le Toullec, and J.-P. Pinceaux, Phys. Rev. B **32**, 7611 (1985).
[3] N. Prokofev and B. Svistunov, Physical review letters **94**, 155302 (2005).
[4] E. Kim and M. Chan, Nature **427**, 225 (2004).
[5] T. Guillot, Planetary and Space Science **47**, 1183 (1999), ISSN 0032-0633.
[6] J. M. McMahon, M. A. Morales, C. Pierleoni, and D. M. Ceperley, Reviews of modern physics **84**, 1607 (2012).
[7] M. A. Morales, E. Schwegler, D. Ceperley, C. Pierleoni, S. Hamel, and K. Caspersen, Proceedings of the National Academy of Sciences **106**, 1324 (2009).
[8] A. Jayaraman, Reviews of Modern Physics **55**, 65 (1983).
[9] P. Loubeyre, R. Le Toullec, and J. P. Pinceaux, Phys. Rev. B **36**, 3723 (1987), URL `https://link.aps.org/doi/10.1103/PhysRevB.36.3723`.
[10] C. Cazorla and D. Errandonea, Phys. Rev. B **81**, 104108 (2010).
[11] C. Cazorla, D. Errandonea, and E. Sola, Phys. Rev. B **80**, 064105 (2009).
[12] A. K. Kleppe, M. Amboage, and A. P. Jephcoat, Scientific Reports **4** (2014).
[13] C. Ji, A. F. Goncharov, V. Shukla, N. K. Jena, D. Popov, B. Li, J. Wang, Y. Meng, V. B. Prakapenka, J. S. Smith, et al., Proceedings of the National Academy of Sciences **114**, 3596 (2017), ISSN 0027-8424.
[14] P. Loubeyre, R. LeToullec, and J. P. Pinceaux, Phys. Rev. B **45**, 12844 (1992).
[15] M. I. M. Scheerboom and J. A. Schouten, Phys. Rev. B **53**, R14705 (1996).
[16] E. W. Knapp and S. F. Fischer, The Journal of Chemical Physics **76**, 4730 (1982).
[17] B. Silvi, V. Chandrasekharan, M. Chergui, and R. D. Etters, Phys. Rev. B **33**, 2749 (1986).
[18] J. M. McMahon and D. M. Ceperley, Phys. Rev. B **85**, 219902 (2012).
[19] N. Nettelmann, B. Holst, A. Kietzmann, M. French, R. Redmer, and D. Blaschke, The Astrophysical Journal **683**, 1217 (2008).
[20] J. P. Perdew, K. Burke, and M. Ernzerhof, Phys. Rev. Lett. **77**, 3865 (1996).
[21] S. Grimme, Journal of Computational Chemistry **27**, 1787 (2006), ISSN 1096-987X.

[22] J. Klime and A. Michaelides, The Journal of Chemical Physics **137**, 120901 (2012).
[23] M. D. Segall, P. J. D. Lindan, M. J. Probert, C. J. Pickard, P. J. Hasnip, S. J. Clark, and M. C. Payne, Journal of Physics: Condensed Matter **14**, 2717 (2002).
[24] H. Y. Geng, Q. Wu, M. Marques, and G. J. Ackland, Physical Beview B p. accepted (2019).
[25] S. Azadi and G. J. Ackland, Physical Chemistry Chemical Physics **19**, 21829 (2017).
[26] Y. A. Freiman, S. M. Tretyak, A. Grechnev, A. F. Goncharov, J. S. Tse, D. Errandonea, H.-k. Mao, and R. J. Hemley, Phys. Rev. B **80**, 094112 (2009).
[27] C. Cazorla and J. Boronat, Phys. Rev. B **91**, 024103 (2015).
[28] R. Turnbull, M.-E. Donnelly, M. Wang, M. Peña Alvarez, C. Ji, P. Dalladay-Simpson, H.-k. Mao, E. Gregoryanz, and R. T. Howie, Phys. Rev. Lett. **121**, 195702 (2018).
[29] H. Mao, R. Hemley, Y. Wu, A. Jephcoat, L. Finger, C. Zha, and W. Bassett, Physical review letters **60**, 2649 (1988).
[30] G. Straty and E. Adams, Physical Review **169**, 232 (1968).
[31] R. Mills, D. Liebenberg, and J. Bronson, Physical Review B **21**, 5137 (1980).
[32] J. P. Hansen and E. L. Pollock, Phys. Rev. A **5**, 2651 (1972).
[33] M. A. Morales, S. Hamel, K. Caspersen, and E. Schwegler, Physical Review B **87**, 174105 (2013).
[34] X. Jiang, Y. Zheng, X.-X. Xue, J. Dai, and Y. Feng, The Journal of Chemical Physics **152**, 074701 (2020).
[35] Y. Wang, X. Zhang, S. Jiang, Z. M. Geballe, T. Pakornchote, M. Somayazulu, V. B. Prakapenka, E. Greenberg, and A. F. Goncharov, The Journal of Chemical Physics **150**, 114504 (2019).
[36] M. W. Wong, Journal of the American Chemical Society **122**, 6289 (2000).
[37] R. T. Howie, I. B. Magdău, A. F. Goncharov, G. J. Ackland, and E. Gregoryanz, Physical review letters **113**, 175501 (2014).
[38] I. B. Magdău and G. J. Ackland, Physical review letters **118**, 145701 (2017).
[39] X. Jiang, Y. Zheng, X.-X. Xue, J. Dai, and Y. Feng, The Journal of Chemical Physics **152**, 074701 (2020).
[40] For example, see Supplementary Materials
[41] C.S. Yoo, private communication